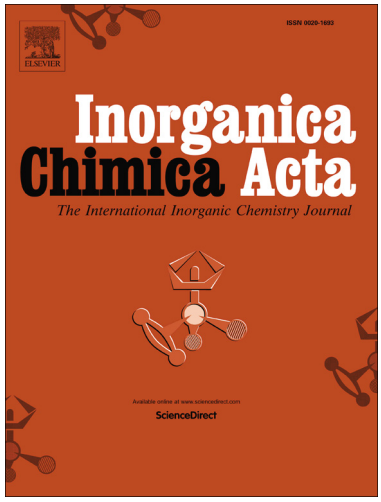

Synthesis, Characterisation and Cytotoxicity Studies of Ruthenium Arene Complexes Bearing Trichlorogermyl Ligands

Connor Deacon-Price, Dario Romano, Tina Riedel, Paul J. Dyson, Burgert Blom

PII: S0020-1693(18)31159-9
DOI: https://doi.org/10.1016/j.ica.2018.09.019
Reference: ICA 18477

To appear in: *Inorganica Chimica Acta*

Received Date: 25 July 2018
Revised Date: 5 September 2018
Accepted Date: 6 September 2018

Please cite this article as: C. Deacon-Price, D. Romano, T. Riedel, P.J. Dyson, B. Blom, Synthesis, Characterisation and Cytotoxicity Studies of Ruthenium Arene Complexes Bearing Trichlorogermyl Ligands, *Inorganica Chimica Acta* (2018), doi: https://doi.org/10.1016/j.ica.2018.09.019

Synthesis, Characterisation and Cytotoxicity Studies of Ruthenium Arene Complexes Bearing Trichlorogermyl Ligands

Connor Deacon-Price,[a] Dario Romano,[b] Tina Riedel,[c] Paul J. Dyson,[c] Burgert Blom *[a]

[a] burgert.blom@maastrichtuniversity.nl

Faculty of Science and Engineering, Maastricht Science Programme (MSP), Maastricht University, P.O. Box 616

6200 MD, Maastricht, the Netherlands

[b] Aachen Maastricht Institute for Biobased Materials

Faculty of Science and Engineering, Maastricht University, Brightlands Chemelot Campus

Urmonderbaan 22, 6167 RD Geleen, the Netherlands

[c] Institut des Sciences et Ingénierie Chimiques,

Ecole Polytechnique Fédérale de Lausanne (EPFL),CH-1015 Lausanne, Switzerland

Keywords: bioorganometallic chemistry • ruthenium complexes • cytotoxicity studies • trichlorogermyl ligand • insertion• group 14 chemistry

Supporting Material is available containing the Cartesian coordinates of the DFT optimised structures.

Abstract: The synthesis of five half sandwich ruthenium(II) trichlorogermyl complexes of the type [(η^6-Arene)Ru(PR_3)Cl($GeCl_3$)] (PR_3 = Phosphane and phosphite ligands; Arene = *p*-cymene or C_6H_5-OC_2H_4OH) is reported: [(η^6-*p*-cymene)Ru($P(OMe)_3$)Cl($GeCl_3$)] (**1**), [(η^6-*p*-cymene)Ru($P(OPh)_3$)Cl($GeCl_3$)] (**2**), [(η^6-*p*-cymene)Ru(PPh_3)Cl($GeCl_3$)] (**3**), [(η^6-*p*-cymene)Ru(pta)Cl($GeCl_3$)] (pta = 1,3,5-triaza-7-phosphaadamantane) (**4**) and [(η^6-C_6H_5-OC_2H_4OH)Ru(pta)Cl($GeCl_3$)] (**5**). The nature of the η^6-arene and phosphane ligand was varied and the complexes have been prepared by facile insertion of $GeCl_2$ (from $GeCl_2$·(dioxane)) into the Ru-Cl bonds of the respective easily accessible precursor complexes [(η^6-Arene)Ru(PR_3)Cl_2]. The

complexes were fully spectroscopically characterized by ^{1}H, $^{13}C\{^{1}H\}$ and $^{31}P\{^{1}H\}$ NMR spectroscopy, UV-Vis, ATR-IR, HRMS (ESI) and their thermal behavior elucidated by TGA. Their cytotoxicity to human ovarian carcinoma (A2780) and non-tumorigenic human embryonic kidney HEK293 cell lines is also reported, and represents the first cytotoxic investigations of Ru(II) germyl complexes to date. The first DFT studies (B3LYP; basis set 6- 31+G(d,p) for H, C, O, P, Cl, N, and Ge atoms and DGDZVP for Ru atom) on trichlorogermyl ruthenium complexes were carried out on complex **2** and **5** in order to gain insights into the bonding situation between Ru and Ge and are reported.

1. Introduction

Cancer is amongst one of the most critical challenges that face society. Approximately 8.2 million deaths worldwide were caused by the disease in 2012 [1]. Of those treated, approximately half will receive some form of chemoradiotherapy [2]. Amongst the most common chemotherapeutic agents are platinum based compounds and half of all cancer patients that undergo chemotherapy will receive treatment with a platinum based antineoplastic agent [3]. Of particular note is the drug *cis*-platin, which has retained its position of prominence since its anticancer properties were discovered almost fifty years ago. [4,5] Despite being one of the most potent anticancer drugs [6], there are several key issues that surround the use of *cis*-platin, and other platinum based antineoplastics in chemotherapy. These include cancer's building resistances [7,8], and the vast array of side effects that they cause [9]. It is apparent that alternatives to platinum based antineoplastics are required, specifically involving in the substitution of platinum for other transition metals [10]. This has led to the development of ruthenium based antineoplastics [11]. These compounds display a variety of advantages over that of platinum based chemotherapeutics. These include a mechanism of action that limits toxicity and maximises specificity [12-20], having ideal ligand exchange rate properties [21-24], and possessing a highly customizable structure in terms of ligand design [25-27].
A promising example of a ruthenium based antineoplastic is RAPTA-C. When given in combination with other anticancer drugs, RAPTA-C is observed to effect a reduction in tumour growth by 80%, in very low dosages with the absence of side effects [28]. Such promising results informed our decision to base new complexes on the structure of RAPTA-C (Chart 1).

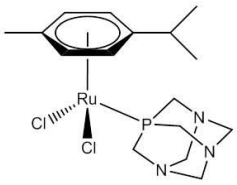

Chart 1. Structure of RAPTA-C, a promising anticancer agent.

It has been found that the presence of trichlorostannyl groups in the ligand sphere of Ru(II) arene complexes can increase the cytotoxicity of ruthenium-arene drugs [29a-b]. Despite these encouraging results, little further work has been reported in this regard. In particular, substitution of Sn with Ge might afford complexes that also exhibit enhanced cytotoxic properties, with the advantage of possibly

being more selective towards cancer cells. To our knowledge, no previous study has been conducted on elucidating the cytotoxicity of ruthenium based complexes bearing germanium ligands in the ligand sphere of Ru(II), and herein we report the first such study. A series of novel trichlorogermyl complexes of the type [(η^6-Arene)Ru(PR_3)Cl($GeCl_3$)] (PR_3 = Phosphane and phosphite ligands; Arene = *p*-cymene or C_6H_5-OC_2H_4OH) have been prepared in a facile way by facile insertion reactions of $GeCl_2$ into the Ru-Cl bonds of easily accessible precursor complexes [(η^6-Arene)Ru(PR_3)Cl_2] affording the complexes [(η^6-Arene)Ru(PR_3)Cl($GeCl_3$)] (Figure 1) [30]. Both arene and phosphane have been modulated and their cytotoxicity towards human ovarian carcinoma (A2780) and non-tumorigenic human embryonic kidney HEK293 cell lines is reported.

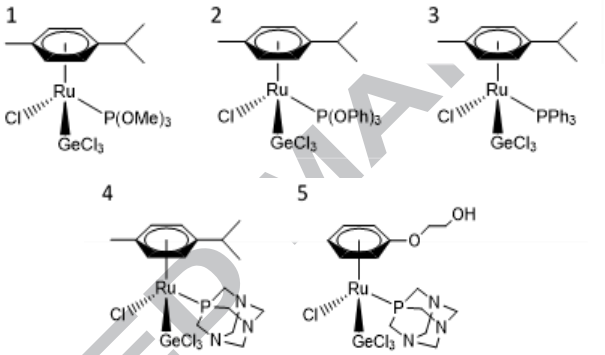

Figure 1. All synthesized complexes in this report (**1** - **5**): **1** – [η^6-*p*-cymene)Ru($P(OMe)_3$)Cl($GeCl_3$)]; **2** – [(η^6-*p*-cymene)Ru($P(OPh)_3$)Cl($GeCl_3$)]; **3** – [(η^6-*p*-cymene)Ru(PPh_3)Cl($GeCl_3$)]; **4** – [(η^6-*p*-cymene)Ru(pta)Cl($GeCl_3$)]; **5** – [(η^6-C_6H_5-OC_2H_4OH)Ru(pta)Cl($GeCl_3$)]. *(Where pta is 1,3,5-triaza-7-phosphaadamantane*,$C_6H_{12}N_3P$).

2. Experimental Section

2.1 General Experimental Section

All experiments and manipulations that involved the germanium(II) chloride dioxane complex (1:1) were performed under anaerobic conditions using a Saffron Scientific Equipment Ltd. DAB01S Glove Box and/or standard Schlenk techniques with dry nitrogen as an inert atmosphere in dried and degassed dichloromethane. All other experiments and manipulations were performed in either dichloromethane, or a mixture of dichloromethane and methanol. Standard workup protocols were

utilized to acquire the desired complexes, with specific reactions shown by scheme 2. All reagents used were purchased from Sigma-Aldrich. [(η^6-*p*-cymene)Ru(P(OMe)$_3$)Cl$_2$] [31] and [(η^6-*p*-cymene)Ru(P(OPh)$_3$)Cl$_2$] [31] which were synthesized in prior experiments by associated research groups within the same laboratory. NMR spectra were recorded using a Bruker UltraShield 300 and Bruker Avance III HD Spectrometer, in WG-1000-7 5mm NMR sample tubes. This hardware was run on and the data acquired processed on Bruker's TopSpin 3.1 software. ^{1}H and ^{13}C{^{1}H} spectra were calibrated using residual solvent peaks for reference, when possible. This was done for all solvents: chloroform-d (δH 7.26 ppm; δC 77.2 ppm), dimethyl sulfoxide-d$_6$ (δH 2.50 ppm; δC 39.5 ppm), and deuterium oxide (δH 4.79 ppm). In cases where complexes were only sparingly soluble filtration was performed to remove any solids, allowing for an entirely liquid phase sample. Abbreviations: s = singlet; d = doublet; t = triplet, q = quartet, ABq = AB quartet; sept = septet; m = multiplet; br = broad; v = very. All coupling constants are quoted in Hz. In the case of broad signals, half height widths ($\Delta\nu_{1/2}$) are also quoted in Hz. Through the use of 2-D spectra, including H,H COSY, H,C HSQC, and H,C HMBC, unambiguous signal assignments can be made. However, it should be noted that not all complexes have had such analysis techniques implemented. A and B superscripts denote diastereotopic groups, often relating to methyl groups present on η^6-*p*-cymene after a group 4 dihalide insertion has been successfully executed. ^{1}H NMR was recorded at 300.1 MHZ, ^{13}C{^{1}H}NMR was recorded at 75.5 MHz, and ^{31}P{^{1}H}NMR was recorded at 121.5 MHz. All NMR results were recorded between 297 K and 301 K. Melting points were acquired through slow heating in capillary tubes using the Stuart SMP10 melting point apparatus. All complex samples undergo decomposition rather than melting, which is denoted as "+ dec.". High resolution Electron Ionisation Spray (ESI) mass spectra were recorded using an Orbitrap LTQ XL of Thermo Scientific mass spectrometer at the Technische Universitaet Berlin. Raw data was evaluated and processed using the X-calibur computer program. In all cases the isotope distribution pattern of the signal was checked against theory . All values reported related to the line of highest intensity. Attenuated total reflection Fourier transform infrared spectroscopy (ATR-FTIR) was carried out using Shimadzu's IRAffinity-1S Fourier Transform Spectrometer coupled with a MIRacle 10 Single Reflection ATR accessory, using Shimadzu's IRsolution (version 1.60) software to analyse and process raw data. Specifications are as follows: % Transmission; Apodization - Happ-Genzel; 64 scans per measurement. Abbreviations: w = weak; m = medium; s = strong; v = very; br = broad.

Background spectra were recorded before measurements were made, using ethanol to prepare the sample area.

Ultraviolet–visible spectroscopy (UV-vis) was recorded using Shimadzu's UV-3600 Plus, UV-vis-NIR Spectrophotometer coupled with LISR-3100 for diffuse reflectance measurement, with raw data being analysed and processed using Shimadzu's UVProbe (version 2.42) software. Scans were run from 750 – 200 nm, with the scan speed set at medium and scan intervals set at 0.5 nm. The solvents used is dependent on the complex being measured, as solubility between complexes can vary widely. Thermogravimetric analysis (TGA) was recorded using TA Instrument's Q500 Thermogravimetric Analyzer, with raw data being analysed and processed using TA Instrument's Universal Analysis 2000 (version 4.5A, build 4.5.0.5) software. Measurements were performed between room temperature and 500 °C, as to exceed this temperature may cause damage to the device.

2.2 Density Functional Theory Calculations

DFT calculations were performed to model the complexes **2** and **5**. Guassian09 software package was used. For all the calculations, the level of theory used for all calculations is B3LYP [40] with the basis set 6- 31+G(d,p) for H, C, O, P, Cl, N, and Ge atoms and DGDZVP for Ru atom. Geometry optimizations were calculated without any constrains. Energies and Natural Bond Order analyses were calculated on the optimized structures.

2.3 Cell culture and inhibition of cell growth

The human A2780 ovarian carcinoma and HEK embryonic kidney cells were obtained from the European Collection of Cell Cultures (Salisbury, U.K.). A2780 and A2780cisR cells were grown routinely in RPMI-1640 medium, while HEK cells were grown in DMEM medium, with 10% fetal bovine serum (FBS) and 1 % antibiotics at 37°C and 5% CO_2. Cytotoxicity was determined using the MTT assay (MTT = 3-(4,5-Dimethyl-2-thiazolyl)-2,5-diphenyl-2H-tetrazolium·bromide). Cells were seeded in 96-well plates as monolayers with 100 µL of cell suspension (approximately 5000 cells) per well and pre-incubated for 24 h in medium supplemented with 10% FBS. Compounds were prepared as DMSO solutions and then dissolved in the culture medium and serially diluted to the appropriate concentration, to give a

final DMSO concentration of 0.5%. 100 µL of the drug solution was added to each well, and the plates were incubated for another 72 h. Subsequently, MTT (5 mg/mL solution) was added to the cells and the plates were incubated for a further 2 h. The culture medium was aspirated, and the purple formazan crystals formed by the mitochondrial dehydrogenase activity of vital cells were dissolved in DMSO. The optical density, directly proportional to the number of surviving cells, was quantified at 590 nm using a multiwell plate reader, and the fraction of surviving cells was calculated from the absorbance of untreated control cells. Evaluation is based on means from at least two independent experiments, each comprising triplicates per concentration level.

2.4 Synthesis of Complex **1** [(η^6-*p*-cymene)Ru($P(OMe)_3$)Cl($GeCl_3$)]:

[Ru(η^6-*p*-cymene)Cl_2{$P(OMe)_3$}] (0.149 g, $3.46x10^{-4}$ mol) was measured within a glovebox under inert N_2 atmosphere, and was subsequently placed in a Schlenk flask. Germanium(II) chloride dioxane complex (1:1) (0.094 g $3.83x10^{-4}$ mol) was then also added to this Schlenk flask. Dried and degassed dichloromethane (~50mL) was added to this vessel *via* syringe, and was agitated by hand. This elicited a colour change from a transparent red solution, to a transparent orange solution within 30 seconds. The vessel was then sealed, removed from the glovebox, and allowed to stir at room temperature under a static N_2 pressure for a further 1.5 hours. No further colour change occurred across this time period. The solvent was then removed *in vacuo* at 40 °C, affording an oily orange substance. Diethyl ether (30 mL) was added to this material in a round bottomed flask, affording an orange precipitate and a solution in which the material was sparingly soluble. In order to solubilise, dichloromethane (10 mL) was added to this solution to produce a 3:1 mixture of diethyl ether: dichloromethane. This orange supernatant was further concentrated *in vacuo* to produce an oily orange substance. Diethyl ether (10 mL) was added to this oily material, producing a red precipitate and a yellow solution. This yellow solution was decanted off, and the precipitate allowed to air dry. This resulted in the formation of a dark orange solid powder. Soluble in chloroform. Air stable. 0.138g of dark orange solid (69%). Melting Point: 132 °C + dec.

^{1}H NMR: (300.1 MHz, $CHCl_3$-d_1, 25°C): δ = 5.92 – 5.84 (m, 4H, η^6-C_6H_4), 3.85 (d, ^3J(H,P) = 11.3 Hz,

9H, P(OCH_3)$_3$), 2.79 (sept, ^3J(H,H) = 7.0 Hz, 1H, CH(CH$_3$)$_2$), 2.12 (s, 3H, CH_3), 1.26 (d, ^3J(H,H) = 5.5 Hz, 3H, CH(CH_3)$_2^A$), 1.23 (d, ^3J(H,H) = 5.4 Hz, 3H, CH(CH_3)$_2^B$). ^{13}C{^{1}H}NMR: (75.5 MHz, $CHCl_3$-d_1, 26°C): δ = 119.4 (d, ^2J(C,P) = 3.9 Hz, η^6-C_6H_4), 103.5 (d, ^2J(C,P) = 1.6 Hz, η^6-C_6H_4), 95.1 (d, ^2J(C,P) = 5.8 Hz, η^6-C_6H_4), 93.5 (d, ^2J(C,P) = 2.1 Hz, η^6-C_6H_4), 91.9 (d, ^2J(C,P) = 9.2 Hz, η^6-C_6H_4), 89.7 (s, η^6-C_6H_4), 54.7 (d, ^2J(C,P) = 7.9 Hz, P(OCH$_3$)$_3$), 30.6 (s, CH(CH$_3$)$_2$), 22.3 (s, CH$_3$), 21.7 (s, CH(CH$_3$)$_2^A$), 18.5 (s, CH(CH$_3$)$_2^B$). ^{31}P{^{1}H}NMR: (121.5 MHz, $CHCl_3$-d_1, 25°C): δ = 125.3 (s). HRMS (ESI (+)) = 502.93904 (63%), 436.03867 (59%), 395.01191 [M-$GeCl_3$]$^+$ (100%) (calc 395.01169). ATR-FTIR: μ(cm^{-1}) = 3071 (w), 2951 (m, Alkyl C-H Stretching), 2870 (w), 2849 (w), 2025 (w), 1931 (w), 1896 (w), 1539 (w, Aromatic C=C Bending), 1506 (w), 1464 (m), 1445 (m), 1375 (w), 1260 (w), 1179 (m, P-O-Me), 1011 (vs, P-O-C), 891 (w), 872 (m), 856 (m, Aromatic C-H Bending), 785 (vs, P-O-C), 737 (vs), 702 (m), 675 (m), 631 (w). TGA: (°C, Weight % decrease): 130 – 193 (18%), 193 – 232 (6%), 260 – 350 (10%). UV/Vis λ_{max} (chloroform): 347.0 nm.

2.5 Synthesis of Complex **2** [(η^6-*p*-cymene)Ru(P(OPh)$_3$)Cl($GeCl_3$)]:

[Ru(η^6-*p*-cymene)Cl_2{P(OPh)$_3$}] (0.150 g, 2.43x10^{-4} mol) was measured within a glovebox under inert N_2 atmosphere, and was subsequently placed in a Schlenk flask. Germanium(II) chloride dioxane complex (1:1) (0.065 g, 2.68x10^{-4} mol) was then also added to this Schlenk flask. Dried and degassed dichloromethane (50 mL) was added to this vessel, which was then agitated, eliciting an immediate colour change from a transparent dark red solution to a transparent yellow solution. This vessel was sealed, and stirred outside of the glovebox for a further 10 minutes. The solvent was removed *in vacuo* at 40 °C until a canary yellow precipitate was formed. This powder was dried *in vacuo* for a further 15 minutes in order to remove excess dioxane, affording a yellow solid. Crystals suitable for single crystal X-ray diffraction analysis were grown from chloroform-d at 7 °C, whilst allowing evaporation to take place._Soluble in dichloromethane, very sparingly soluble in chloroform. Air stable. 0.101g of canary yellow solid (54%). Melting Point: 224 °C + dec. ^{1}H NMR: (300.1 MHz, $CHCl_3$-d_1, 24°C): δ = 7.32 – 7.19 (m, 15H, P(OPh)$_3$), 5.88 – 5.39 (m, 4H, η^6-C_6H_4), 2.64 (sept, ^3J(H,H) = 6.9 Hz, 1H, CH(CH$_3$)$_2$), 2.03 (s, 3H, CH_3), 1.19 (d, ^3J(H,H) = 6.9 Hz, 3H, CH(CH_3)$_2^A$), 1.08 (d, ^3J(H,H) = 7.0 Hz, 3H, CH(CH_3)$_2^B$). *No $^{13}C\{^1H\}$NMR is available due to low solubility*. ^{31}P{^{1}H}NMR: (121.5 MHz, $CHCl_3$-d_1, 25°C): δ = 116.7 (s). HRMS (ESI (+)) = 670.97637

(100%), 622.97609 (4%), 318.18591 (6%), 282.27971 (9%) ATR-FTIR: μ(cm^{-1}) = 3065 (w), 2955 (w), 2922 (m, Alkyl C-H Stretching), 2853 (w), 1587 (m, Aromatic C=C Bending), 1485 (s), 1454 (m), 1393 (w), 1261 (m), 1207 (s), 1186 (vs, P-O-Ar), 1152 (s), 1088 (m), 1053 (m), 1026 (s), 1007 (m). 949 (vs), 908 (vs), 893 (vs), 874 (s, P-O), 802 (s, P-O-C), 775 (vs), 766 (vs), 737 (s), 719 (s), 685 (vs). TGA: (°C, Weight % decrease): 207 – 250 (16%), 250 – 371 (22%), 371 – 492 (21%). UV/Vis λ_{max} (dichloromethane): 438.5 nm. Connectivity confirmed by single crystal X-ray diffraction analysis of single crystals (low quality data set. Omitted from discussion).

2.6 Synthesis of Complex **3** [(η^6-*p*-cymene)Ru(PPh_3)Cl($GeCl_3$)]:

Dichloro(*p*-cymene)ruthenium(II) dimer (0.509 g, $8.31x10^{-4}$ mol) was measured and added to triphenylphosphine (3.268 g, $1.25x10^{-2}$ mol) in a round bottomed flask. Dichloromethane (50 mL) was added to this vessel, and the reaction mixture was stirred under reflux (50 °C) for 3 hours. No colour change occurred across the duration of this reaction, remaining a transparent dark red solution throughout. The solvent was removed *in vacuo* at 40 °C to a highly concentrated solution (~8 mL). Diethyl ether (50 mL) was added to this solution, causing the product to precipitate out of solution, and the supernatant was subsequently decanted off. This was repeated four more times until the decanted supernatant was colourless. A dark red crystalline material was obtained, and was allowed to air dry for 1 hour before proceeding with analysis and further reactions. A yield of 0.748 g ($1.32x10^{-3}$ mol, 79.2%) was recorded.

This product, [Ru(η^6-*p*-cymene)Cl_2(PPh_3)], (0.300 g, $5.28x10^{-4}$ mol) was added to a Schlenk flask within a glovebox under an inert N_2 atmosphere. Germanium(II) chloride dioxane complex (1:1) (0.129 g, $5.55x10^{-4}$ mol) was then added to this vessel, which was then sealed and placed on a Schlenk line. Dried and degassed dichloromethane (20 mL) was added to this vessel This reaction mixture was allowed to stir for 15 minutes. The solution went from a transparent cabernet red to a transparent amber solution in approximately 1 minute. This solvent was then concentrated *in vacuo* at 40 °C to form a highly concentrated solution (~5 mL), until the point of insipience was reached. This solution was allowed to rest, before decanting the supernatant off, leaving behind an orange-red semi-crystalline residue. This material was then dried *in vacuo* for 15 minutes at room temperature. Soluble in dichloromethane, sparingly soluble in chloroform and dimethyl sulfoxide. Air stable. 0.238 g

of orange-red solid (63%). Melting Point: 124 °C + dec.^{1}H NMR: (300.1 MHz, $CHCl_3$-d_1, 25°C): δ = 7.66 – 7.23 (m, 15H, PPh_3), 6.10 (d, ^{3}J(H,H) = 6.1 Hz, 1H, η^{6}-C_6H_4), 5.68 (d, ^{3}J(H,H) = 5.9 Hz, 1H, η^{6}-C_6H_4), 5.39 (d, ^{3}J(H,H) = 5.9 Hz, 1H, η^{6}-C_6H_4), 4.79 – 4.77 (m, 1H, η^{6}-C_6H_4), 2.70 (sept, ^{3}J(H,H) = 6.9 Hz, 1H CH(CH_3)$_2$), 1.52 (s, 3H, CH_3), 1.21 (d, ^{3}J(H,H) = 6.9 Hz, 3H, CH(CH_3)$_2^{A}$), 1.16 (d, ^{3}J(H,H) = 6.9 Hz, 3H, CH(CH_3)$_2^{B}$). ^{13}C{^{1}H}NMR: (75.5 MHz, $CHCl_3$-d_1, 26°C, ppm): δ = 133.4 (d, ^{x}J(C,P) = 9.9 Hz, $C^{2,6}$ or $C^{3,5}$ PPh_3), 132.6 (d, ^{1}J(C,P) = 48.0 Hz, C^{1} PPh_3), 129.6 (d, ^{4}J(C,P) = 2.5 Hz, C^{4} PPh_3), 127.3 (d, ^{x}J(C,P) = 10.3 Hz, $C^{2,6}$ or $C^{3,5}$ PPh_3), 98.0 (s, η^{6}-C_6H_4), 94.2 (d, ^{2}J(C,P) = 3.4 Hz, η^{6}-C_6H_4), 92.7 (s, η^{6}-C_6H_4), 88.0 (s, η^{6}-C_6H_4), 87.4 (s, η^{6}-C_6H_4), 87.3 (s, η^{6}-C_6H_4), 29.3 (s, CH(CH_3)$_2$), 21.2 (s, CH(CH_3)$_2^{A}$), 20.7 (s, CH(CH_3)$_2^{B}$), 15.9 (s, CH_3). ^{31}P{^{1}H}NMR: (121.5 MHz, $CHCl_3$-d_1, 26°C): δ = 28.9 (s). ^{31}P{^{1}H}NMR: (121.5 MHz, DMSO-d_6, 26°C, ppm): δ = 32.9 (s, exchanged, 30%), 29.3 (s, product, 70%). HRMS (ESI (+)) = 706.99000 (2%), 682.02768 (16%), 668.99667 (100%), 641.00159 (16%), 574.10092 (6%), 533.07416 [M-$GeCl_3$]$^{+}$ (calc 533.07388) (24%), 279.09349 (6%). ATR-FTIR: μ(cm^{-1}) = 2988 (m), 2970 (m), 2901 (m, Alkyl C-H Stretching), 2872 (m), 2361 (m), 2322 (m), 1977 (w), 1558 (w), 1541 (w), 1506 (m, Aromatic C=H Bending), 1487 (w), 1472 (m), 1456 (m), 1433 (s), 1395 (w), 1375 (m), 1339 (w), 1314 (w), 1260 (m), 1182 (w), 1159 (w), 1090 (vs), 1059 (s), 1028 (s), 1001 (m), 972 (w), 924 (w), 901 (w), 860 (m), 845 (w), 799 (s, Aromatic C=C Bending), 746 (vs), 691 (vs), 669 (m, P-C), 631 (s), 617 (w). TGA: (°C, Weight % decrease): 222 – 254 (12%), 254 – 287 (4%), 287 – 373 (19%), 373 – 493 (16%). UV/Vis λ_{max} (dichloromethane): 358.0 nm.

2.7 Synthesis of Complex **4** [(η^{6}-*p*-cymene)Ru(pta)Cl($GeCl_3$)]:

Germanium(II) chloride dioxane complex (1:1) (0.108 g, 4.67x10^{-4} mol) was measured in to a Schlenk flask within a glove box. [Ru(η^{6}-*p*-cymene)Cl_2(pta)] (0.206 g, 4.45x10^{-4} mol) was then added to this vessel. Dried and degassed dichloromethane (50 mL) was added to the vessel *via* syringe, to dissolve the reagents. This produced a transparent red solution. This reaction mixture was stirred at room temperature for 1 hour, forming a translucent orange solution. The solvent was removed from the vessel *in vacuo* at 40 °C. This produced an orange powder. Soluble in dimethyl sulfoxide, water, and chloroform. Air stable. 0.201 g of orange solid (76%). Melting Point: 172 °C + dec.^{1}H NMR: (300.1 MHz, H_2O-d_2, 25°C): δ = 6.33 – 5.65 (m, 4H, η^{6}-C_6H_4), 4.87 (br s, 6H, NCH_2N), 4.45 – 4.32 (m, 6H, PCH_2N), 2.50 (sept, ^{3}J(H,H) = 6.8 Hz, 1H, CH(CH_3)$_2$), 2.01 (s, 3H,

C*H*$_3$), 1.13 (d, ^3J(H,H) = 6.8 Hz, 6H, CH(C*H*$_3$)$_2$) (These signals correspond to the exchanged product). ^{13}C{^{1}H}NMR: (75.5 MHz, DMSO-d_6, 25°C, ppm): δ = 70.7 (s, N*C*H$_2$N), 66.8 (s, P*C*H$_2$N), 30.7 (s, *C*H(CH$_3$)$_2$), 24.5 (s, CH(*C*H$_3$)$_2$), 22.2 (d, ^3J(C,P) = 36.3 Hz, CH(*C*H$_3$)$_2$), 18.8 (s, *C*H$_3$) (Aromatic signals not visible, due to low signal to noise ratio). ^{13}C{^{1}H}NMR: (75.5 MHz, H$_2$O-d_2, 28°C): δ = 116.9 (s, η^6-*C*$_6$H$_4$), 101.2 (s, η^6-*C*$_6$H$_4$), 94.6 (d, ^2J(C,P) = 3.5 Hz, η^6-*C*$_6$H$_4$), 91.4 (d, ^2J(C,P) = 2.8 Hz, η^6-*C*$_6$H$_4$), 88.9 (d, ^2J(C,P) = 4.9 Hz, η^6-*C*$_6$H$_4$), 88.0 (s, η^6-*C*$_6$H$_4$), 70.9 (d, ^3J(C,P) = 5.3 Hz, N*C*H$_2$N), 66.6 (s, P*C*H$_2$N), 30.8 (s, *C*H(CH$_3$)$_2$), 22.1 (s, CH(*C*H$_3^A$)$_2$), 21.0 (s, CH(*C*H$_3^B$)$_2$), 18.7 (s, *C*H$_3$) (These signals correspond to the exchanged product). ^{31}P{^{1}H}NMR: (121.5 MHz, CHCl$_3$-d_1, 25°C): δ = -36.0 (v br s, $\Delta\nu_{1/2}$ = 40.5 Hz). ^{31}P{^{1}H}NMR: (121.5 MHz, H$_2$O-d_2, 26°C): δ = -19.1 (s, exchanged, 96%), -28.1 (s, unexchanged product, 4%). HRMS (ESI (+)) = 577.01601 (100%), 544.00013 (30%), 535.98937 [M-HCl-Cl]$^+$ (calc 535.94184) (41%), 466.03814, (17%), 428.06163 [M-GeCl$_3$]$^+$ (calc 428.05962) (51%), 312.01077 (2%), 229.17127 (6%). ATR-FTIR: μ(cm^{-1}) = 2963 (m, Alkyl C-H Stretching), 2903 (w), 1624 (w, Aromatic C=C Bending), 1541 (w), 1506 (w), 1449 (w), 1406 (w), 1389 (w), 1304 (w), 1260 (vs), 1219 (w, C-N), 1080 (vs), 1018 (vs), 984 (s), 951 (s), 939 (s), 887 (m), 870 (s, Aromatic C-H Bending), 795 (vs), 772 (vs), 729 (m, P-C), 662 (m), 631 (m), 610 (m). TGA: (°C, Weight % decrease): 85 – 195 (7%), 195 – 275 (11%), 275 -387 (10%), 387 – 489 (17%). UV/Vis λ_{max} (water): 404.0 nm.

2.8 Synthesis of Complex **5** [(η^6-C$_6$H$_5$-OC$_2$H$_4$OH)Ru(pta)Cl(GeCl$_3$)]:

A slightly altered version of the methods demonstrated Matsinha, *et. al.,* was used to synthesise this complex. [29d] Dichloro(η^6-2-phenoxyethanol)ruthenium(II) dimer (0.556 g, 1.02 mmol) was measured and dissolved in a 1:1 dichloromethane: methanol solution (50 mL). 1,3,5-triaza-7-phosphaadamantane (0.328 g, 2.09 mmol) was added to this mixture, and was then stirred at 50 °C for 30 minutes. The solution started as a brown colour, and became darker brown as the reaction proceeded. The solvent was then removed *in vacuo* at 40 °C giving a brick orange precipitate. This material was dissolved in a hot 1:1 dichloromethane: methanol solution (100 mL) and allowed to stand for 2 hours. This gave a black precipitate, which was separated from the orange solution *via* vacuum filtration. The filtrate was then concentrated *in vacuo* at 40 °C until the point of insipience was reached. The red-orange supersaturated solution was then placed at -25 °C for 16 hours. The supernatant was decanted affording a burnt orange precipitate. This precipitate was washed with diethyl ether (10 mL).

This powder dried *in vacuo* for 2 h, affording the precursor [Ru(η^6-2-phenoxyethanol)Cl_2(pta)]. [Ru(η^6-2-phenoxyethanol)Cl_2(pta)] (0.142 g, 3.05x10^{-4} mol) was then weighed into a Schlenk tube in a glove with germanium(II) chloride dioxane complex (1:1) (0.074 g, 3.20x10^{-4} mol). then dissolved in dichloromethane (20 mL). The reaction was stirred for 18 h at room temperature. The materials are only sparingly soluble in dichloromethane, resulting in a translucent orange solution. This solution became slightly lighter in colour after this reaction period, yet remained translucent. The mixture was then vacuum filtered, yielding an orange precipitate as product which was dried *in vacuo*. Soluble in dimethyl sulfoxide, and water. Air stable. 0.097g of orange solid (52%). Melting Point: 174 °C + dec. ^{1}H NMR: (300.1 MHz, H_2O-d_2, 27°C): δ = 6.09 – 5.85 (m, 3H, η^6-C_6H_5), 5.56 (d, ^3J(H,H) = 6.4 Hz, 1H, η^6-C_6H_5), 5.19 (t, ^3J(H,H) = 5.4 Hz, 1H, η^6-C_6H_5), 4.88 (s, 6H, NCH_2N), 4.83 (s, 1H, O*H*), 4.39 (s, 6H, PCH_2N), 4.24 (t, ^3J(H,H) = 5.2 Hz, 2H, η^6-ArOCH_2), 3.90 (t, ^3J(H,H) = 5.2 Hz, 2H, CH_2CH_2OH) (These are the signals of the unexchanged product, other signals visible in the baseline corresponding to the exchanged product). ^{13}C{^{1}H}NMR: (75.5 MHz, DMSO-d_6, 28°C): δ = 159.1 (s, η^6-C_6H_5), 141.5 (d, ^3J(C,P) = 3.0 Hz, η^6-C_6H_5), 129.9 (s, η^6-C_6H_5), 120.9 (s, η^6-C_6H_5), 114.9 (s, η^6-C_6H_5), 91.3 (s, η^6-C_6H_5), 71.0 (s, NCH_2N), 69.8 (s, $PhOCH_2$), 60.0 (s, CH_2CH_2OH), 59.5 (s, PCH_2N) (signals corresponding to unexchanged product). ^{31}P{^{1}H}NMR: (121.5 MHz, H_2O-d_2, 27°C): δ = -16.9 (exchanged, 22%), -23.9 (s, unexchanged, 78%). ^{31}P{^{1}H}NMR: (121.5 MHz, DMSO-d_6, 27°C): δ = -22.7 (s). HRMS (ESI (+)) = 467.99483 (11%), 432.01808 $[M\text{-}GeCl_3]^+$ (calc 432.01816) (100%), 402.00744, (2%), 315.96757 (6%). ATR-FTIR: μ(cm^{-1}) = 3362 (v br w, OH), 3075 (w), 2961 (w, Alkyl C-H Stretching), 1626 (w), 1524 (vs), 1447 (s), 1410 (m), 1304 (m), 1261 (vs), 1219 (m, C-N), 1144 (w), 1115 (m), 1082 (s), 1053 (m), 1024 (vs), 982 (vs), 947 (s), 939 (vs), 908 (s), 897 (s), 837 (vs, Aromatic C-H Bending), 812 (vs), 770 (vs), 743 (s, P-C), 727 (s), 660 (vs), 608 (m). TGA: (°C, Weight % decrease): 157 – 201 (4%), 201 – 272 (9%), 272 – 431 (19%), 431 – 495 (6%). UV/Vis λ_{max} (dimethyl sulfoxide,): 346.5 nm.

3. Results and Discussion

Literature procedures were followed for the synthesis of the pta precursor complexes [(η^6-*p*-cymene)Ru(pta)Cl_2], and [(η^6-C_6H_5-OC_2H_4OH)Ru(pta)Cl_2], with only slight modifications. [29c-e] [(η^6-*p*-cymene)$RuCl_2]_2$ was cleaved with two molar equivalents of $P(OMe)_3$, PPh_3 and $P(OPh)_3$ affording the precursors [(η^6-*p*-cymene)Ru(PR_3)Cl_2] (PR_3 = $P(OMe)_3$, PPh_3 and $P(OPh)_3$), also prepared using standard literature procedures [31]. These easily accessible half sandwich ruthenium(II) dichloride complexes were subsequently treated with $GeCl_2$(dioxane) in a 1:1 ratio, typically in dichloromethane affording, by facile $GeCl_2$ insertion into the Ru-Cl bonds of the respective precursor complexes, the novel trichlorogermyl half-sandwich complexes **1**-**5** (Scheme 1) selectively [30]. The complexes **1**-**5** are remarkably stable and can be handled in air without any noticeable decomposition taking place. This suggests that the trichlorogermyl ligand is stable to hydrolysis on coordination to the Ru centre.

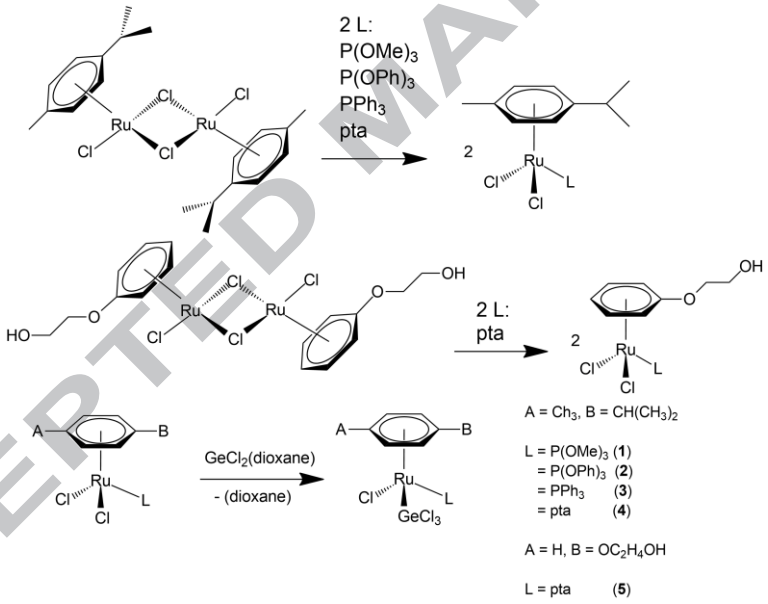

Scheme 1. Top and middle: Cleavage of Ru(II) dimer complexes to produce the known piano-stool precursors. Bottom: Insertion of $GeCl_2$ into the Ru-Cl bonds of precursors from **I** and **II** yielding target complexes **1** – **5**.

The trichlorogermyl complexes were isolated with moderate to high yields (54 – 76 %) and ranged in colour from canary-yellow to orange red.

^{1}H NMR spectroscopy proved an exceptionally useful tool for confirming the insertion of the $GeCl_2$ into the Ru-Cl bonds of the precursor complexes to afford the Ru-$GeCl_3$ moiety. In particular for the

complexes bearing the *p*-cymene ring (**1**-**3**), the insertion of the $GeCl_2$ renders the CH_3 groups of the ^{i}Pr on the p-cymene ring diastereotopic and two sets of resonance signals are observed for $CH(CH_3^A)(CH_3^B)$, with a common cross peak in the two dimensional H,H-COSY spectrum for these resonance signals to the methine proton $CH(CH_3^A)(CH_3^B)$. In complex **4** these signals are isochronous in H_2O-d_2. A similar picture emerges in the $^{13}C\{^1H\}$ NMR spectra of complexes **1**-**4**, where again two sets of resonance signals are observed for the diastereotopic $CH(CH_3^A)(CH_3^B)$ methyl groups. This is in contrast to the starting materials for complexes **1**-**4** *i.e.* $[(\eta^6\text{-p-cymene})Ru(PR_3)Cl_2]$, where the ^{i}Pr groups are not diastereotopic and typically feature one resonance signal for both equivalent $CH(CH_3)_2$. In addition, the presence of a $GeCl_3$ ligand on the Ru(II) centre typically results in six resonance signals for the coordinated arene ring in the $^{13}C\{^1H\}$ NMR spectra, due to loss of symmetry in the complexes. In most cases for these resonance signals, a $^2J(C,P)$ coupling is observed to the Ru(II) bound phosphane ligand.

The presence of phosphane or phosphite ligands in complexes **1**-**5** provided a further instructive spectroscopic handle to track the completion of the reactions and a comparison to their respective precursor complexes ($[(\eta^6\text{-Arene})Ru(PR_3)Cl_2]$), prior to $GeCl_2$ insertion (Table 1).

Table 1. Summary of $^{31}P\{1H\}$NMR data with different solvents ("X" indicates a solvent which was not used for measurement of a complex. Round brackets indicate the ligand exchange product).

$^{31}P\{^1H\}$NMR	$CHCl_3$-d_1	DMSO-d_6	H_2O-d_2
1	125.3	X	X
2	116.7	X	X
3	28.9	29.3 (32.9)	X
4	-36.0	X	-28.1 (-19.1)
5	X	-22.7	-23.9 (-16.9)

For example: Complex **1** features a singlet resonance signal in the $^{31}P\{^1H\}$ NMR spectrum (δ = 125.3 ppm) which is shifted downfield from its precursor complex $[(\eta^6\text{-}p\text{-cymene})\ Ru(P(OMe)_3)Cl_2)]$ (δ = 115.9 ppm) [31]. Similarly, the precursor complex of **2:** $[(\eta^6\text{-}p\text{-cymene})Ru(P(OPh)_3)Cl_2]$ (δ = 104.2 ppm), [31] has a resonance signal that is upfield shifted from **2**. This relates to a downfield chemical

shift of 9.4 ppm and 12.5 ppm respectively in **1** and **2** due to the deshielding effect of the $GeCl_3$ ligand. Similarly, [(η^6-*p*-cymene)Ru(PPh_3)Cl_2], the precursor to complex **3**, features a resonance signal at δ = 24.1 ppm [32], whilst **3** is shifted downfield by 5.4 ppm (δ = 28.9 ppm). The $^{31}P\{^1H\}$ NMR spectra of some complexes (**3 – 5,** those soluble in these solvents) were also recorded in coordinating H_2O-d_2 and DMSO-d_6 and showed two sets of resonance signals: one high field shifted signal corresponding the unexchanged species, and a low field shifted signal likely corresponding to a ligand exchange product. This is likely due to ligand exchange facilitated by the coordinating solvent, affording species of the type [(η^6-arene)Ru(PR_3)D:($GeCl_3$)]$^+Cl^-$ or [(η^6-arene)Ru(PR_3)D:Cl]$^+GeCl_3^-$ (D: = H_2O-d_2 or DMSO-d_6) [33,34]. Another possible explanation for the presence of two resonance signals is potential hydrolysis of the hydrolytically sensitive Ge-Cl bonds in the $GeCl_3$ moiety affording other species, potentially: [(η^6-arene)Ru(PR_3)Cl($Ge(OD)_3$)]. The latter is unlikely and was ruled out by hydrolysis experiments (see below). Attempts at isolating the exchange species was unsuccessful. Notably, Complex **4**, [(η^6-*p*-cymene)Ru(pta)Cl($GeCl_3$)], displays a significant increase in the exchange product ratio, with approximately 96% of the complex forming the exchange product, whilst only 4% of the unexchanged complex remains (in H_2O-d_2). In complex **5** the ratio is 78 % unexchanged to 22 % exchanged, indicating that it is more stable to aquation (ligand exchange). Hydrolytic stability is known to be an important factor in anticancer agents [37-39].

The species appear to be in equilibrium with each other (exchanged : non-exchanged) as following the ^{31}P NMR spectra over time (several hours) revealed no change in the relative intensities of the respective species.

The complexes were found to be thermally robust with decomposition temperatures in all cases above 100 °C: (**1**: 132, **2**: 224, **3**: 124, **4**: 172, **5**: 174 ºC). TGA was also conducted on all complexes in order to further elucidate their thermal behavior with a view of trying to establish their modes of decomposition thermally. The η^6-*p*-cymene groups can be seen as the 16% loss in complex **2**, and the 19% loss in complex **3**. Phenyl groups from triphenylphosphane correspond to a 12% loss in complex 3. It is difficult to label any further fragment losses with confidence given the fact that many fragments share similar molecular weights. Nevertheless these results underline the robust nature of the complexes, thermally.

In order to preclude the presence of any hydrolysis on the $GeCl_3$ ligand in the complexes, solid-state ATIR spectroscopy was conducted on all complexes. A Ge-OH stretching vibration is expected at 3571 cm^{-1} [36 a, c] which is not detected in any of the complexes. In fact, for complexes **1**-**4** the highest wavenumber stretching vibration is close to ca. 3000 cm^{-1} clearly indicative of no Ge-OH present, further providing evidence for the robust nature of the $GeCl_3$ ligand. In complex **5** a stretching vibration at 3362 cm^{-1} is observed corresponding to the pendant OH group on the alkyl chain attached to the aryl ring.

Solution UV-Vis spectroscopy was conducted on all complexes showing some large variations on the absorption band positions: (**1**: 347, **2**: 438.5, **3**: 358, **4**: 404, **5**: 346.5 nm).

.

Surprisingly, trichlorogermyl ruthenium complexes (complexes of the type $L_nRu\text{-}GeCl_3$; L_n = Ligand sphere) have escaped investigations by DFT studies, and we carried out such an analysis for complexes **2** and **5**. The DFT optimized structure for complex **2** can be found in figure 2, while a visual representation of the frontier orbitals for complex **2** can be found in figure 3. Similar representations for complex **5** can be found in the supporting information.

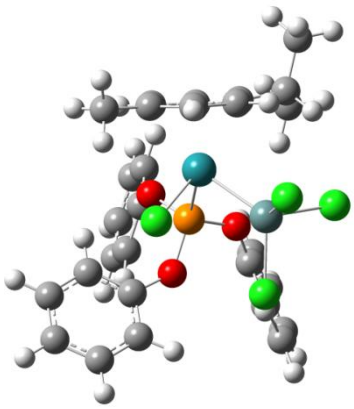

Figure 2. Optimized structure for complex 2. (DFT, B3LYP; basis set 6- 31+G(d,p) for H, C, O, P, Cl, Ge atoms and DGDZVP for Ru atom). (Cyan = Ru, Olive-green = Ge, Green = Cl, Grey = C, Red = O, Orange = P, White = H).

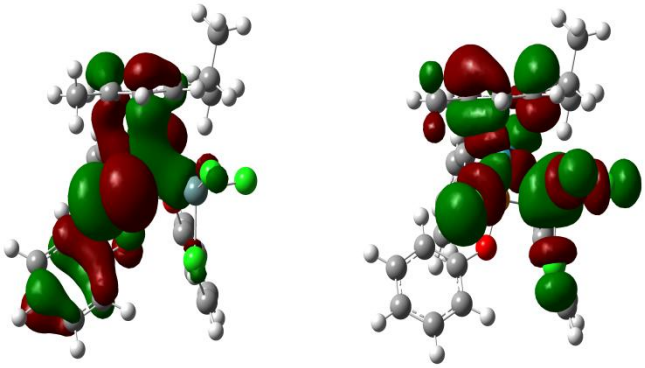

Figure 3. HOMO (left) and LUMO (right) for complex **2**. (B3LYP; basis set 6- 31+G(d,p) for H, C, O, P, Cl, Ge atoms and DGDZVP for Ru atom). Energy of the HOMO is -6.08 eV. Energy of the LUMO is -2.39 eV.

From figure 3 (left) it is possible to visualize that most of the electron density of the HOMO is delocalized on the arene to the ruthenium and germanium together with a significant localization also on the chlorine bound to the ruthenium; while the LUMO is mostly located on the germanium-chloride atoms and the arene centre, with some delocalisation over the coordinated arene ring.

Natural bond analysis (NBO) was calculated to establish the nature of bonds with particular focus on the ruthenium-germanium atoms and bond. Table 2 summarizes the DFT results of the natural bond order analysis for complexes **2** and **5**.

Table 2. Natural bond order analysis for complexes **2** and **5**. (B3LYP; basis set 6- 31+G(d,p) for H, C, O, P, Cl, N, Ge atoms and DGDZVP for Ru atom).

Atom	Bond Polariz. (%)	s-character (%)	p-character (%)	d-character (%)	NBO Charge
			Complex 2		
Ru	47.22	23.72	23.26	53.02	- 0.707
Ge	52.78	76.40	23.36	0.24	+1.247
			Complex 5		
Ru	51.67	24.12	22.51	53.37	- 0.648
Ge	48.33	43.77	55.86	0.36	+1.249

The Wiberg index (WBI) for the Ru-Ge bond calculated for complex **2** is 0.76 while for complex **5** is 0.78, so they are comparable to each other within narrow limits and slightly less than 1. In both

complexes the Ge atom features a somewhat positive NBO charge and the Ru-Ge bonds are slightly polarized in both complexes. Moreover, complex **5** features a higher degree of p-orbital mixing in Ge (55.86 %) compared to only 23.36 % in complex **2** where the latter has more s-character. This variation is indeed surprising given the similar nature of the complexes studied, and suggests that the nature of the other ligands plays a role in the nature of the Ru-Ge bond..

Considering the fact that the LUMO is to a large extent localised, in both complexes on the Ge-Cl bonds in the $GeCl_3$ ligand (Figure 3), this might imply that there is a potential risk of hydrolysis to form Germanium hydroxide species, as Ge-Cl bonds are known to be somewhat hydrolytically labile.[35] In order to probe this potential hydrolytic sensitivity towards the Ge-Cl bonds in the $GeCl_3$ moiety, a simple experiment was conducted whereby a sample of complex **4** was dissolved in water and ^{1}H NMR spectra recorded after stirring and removal of the solvent. No evidence of any Ge-O*H* resonance signals were detected in the ^{1}H NMR spectra, even at very high concentrations and a high number of scans, indicating that hydrolysis of the $GeCl_3$ does not occur. Typically, the Ge-OH group is visible in ^{1}H NMR spectra, in metal bound germyl complexes and even Ge(II) hydroxy species that are not coordinated to transition metals [36].

In vitro cytotoxicity testing of complexes **1-5** were performed on human ovarian carcinoma A2780 and non-tumorigenic human embryonic kidney HEK293 cell lines (Table 3). Complexes **3** and **5** showed some activity with IC50 values of 183 ± 5 and 111 ± 1 on A2780 cells, respectively. Comparable activity was observed for **3** on HEK293 cells. Notably, complex **5** showed some selectivity towards the cancer cell line A2780 with a twice higher activity on cancer cells compared to non-tumorigenic HEK293 cells. Complex **2** was insoluble in any solvent (DMF, DMEM or PBS) compatible with biological medium, therefore, the cytotoxicity test could not be performed for this compound. Complexes **1** and **4** were non-cytotoxic up the measured concentration of 1000uM. Compared to cisplatin, complexes **3** and **5** are approximately 100 times less active. The apparent lack of cytotoxicity **1** and **4** and low activity of **3** and **5** is surprising, given the previous promising results with $SnCl_3$ in the coordination sphere of Ru arene complexes[29a,b]. Obviously, replacing $SnCl_3$ by $GeCl_3$ leads to a loss in cytotoxic activity, which might be due to the fact that the presence of the $GeCl_3$ ligand leads to rapid aquation (see above) and hydrolytic instability, which is known to play a role in cytotoxicity [37-

39]. It is tempting to speculate that complex **5** features a much higher cytotoxicity compared to complex **4** which might be due to its higher stability towards aquation (see above). The complete loss of cytotoxicity in **4** vs **5** despite similar solubility properties potentially underlines the importance of rate of aquation, and since in **4** this is very rapid, might lead to decrease in cytotoxicity.

Table 3. IC50 values of all complexes and cisplatin in either DMF or DMEM (Dulbecco modified eagle medium) solvent on A2780 and HEK cells.

Complex	Solvent	IC50 (A2780)	IC50 (HEK)
1	DMF	> 1000	> 1000
2	Insoluble	N/A	N/A
3	DMF	183 ± 5	146 ± 32
4	DMF	> 1000	> 1000
5	DMEM	111 ± 1	207 ± 22
*cis*platin	DMEM	1.5 ± 0.1	7 ± 1

4. Conclusions

Facile entry into a range of half sandwich ruthenium(II)-arene complexes bearing trichlorogermyl groups was enabled through facile insertion reactions of $GeCl_2$ into the Ru-Cl bonds of readily accessible precursor complexes. The resulting complexes were found to be thermally stable and stable in air, and shown in some cases to undergo rapid aquation or ligand substitution in coordinating solvents. The complexes were fully characterised by a range of spectroscopic methods and by DFT methods, and the first cytotoxic tests of Ru(II) germyl complexes to date were carried out for all 5 complexes on the A2780 and HEK cell lines showing only very weak cytotoxicity. The low cytotoxicity in this class of compound is at odds with analogous trichlorostannyl complexes, and might be as a result of enhanced aquation kinetics which are known to decrease cytotoxicity in biological systems [37-39]. Hence trichlorogermyl ligands in the coordination sphere of Ru(II) are not suitable for anticancer agents based on Ru(II) arene complexes.

5. Acknowledgements

The authors would like to thank the Maastricht Science Programme (MSP) and Maastricht University for financial support of this research. We would also like to thank Dr. M. Schlangen (TU-Berlin, Germany) for the HRMS data.

6. References

[1] World Health Organization, *Monitoring health for the SDGs sustainable development goals,* Geneva, **2016**.

[2] F. G. Herrera, J. Bourhis, G. Coukos, in *CA: Cancer J. Clin*. **2017**, *Vol. 2*, *67*, 65-85.

[3] M. Galanski, M. A. Jakupec, B. K. Keppler, *Curr. Med. Chem.* **2005**, *12*, 2075-2094.

[4] B. Rosenberg, L. VanCamp, J. E. Trosko, V. H. Mansour, *Nature* **1969**, *222*, 385-386.

[5] World Health Organisation, *WHO Model List of Essential Medicines*, **2015**.

[6] Z. H. Siddik, *Oncogene* **2003**, *22*, 7265-7279.

[7] G. Housman, S. Byler, S. Heerboth, K. Lapinska, M. Longacre, N. Snyder, S. Sarkar, *Cancers* **2014**, *6*, 1769-1792.

[8] E. Tsvetkova, G. D. Goss*, Curr. Oncol.* **2012**, *19*, S45-S51.

[9] L. Astolfi, S. Ghiselli, V. Guaran, M. Chicca, E. D. I. Simoni, E. Olivetto, G. Lelli, A. Martini*, Oncol. Rep.* **2013**, *29*, 1285-1292.

[10] I. Ott, R. Gust, *Arch. Pharm.* **2007**, *340*, 117-126.

[11] G. Sava, A. Bergamo, in *Platinum and Other Heavy Metal Compounds in Cancer Chemotherapy: Molecular Mechanisms and Clinical Applications*, Totowa, NJ, **2009**, DOI: 10.1007/978-1-60327-459-3_8, pp. 57-66.

[12] H. Ludwig, R. Evstatiev, G. Kornek, M. Aapro, T. Bauernhofer, V. Buxhofer-Ausch, M. Fridrik, D. Geissler, K. Geissler, H. Gisslinger, E. Koller, G. Kopetzky, A. Lang, H. Rumpold, M. Steurer, H. Kamali, H. Link, *Wien. Klin. Wochenschr.* **2015**, *127*, 907-919.

[13] F. Kratz, L. Messori, *J. Inorg. Biochem*. **1993**, *49*, 79-82.

[14] D. Hogemann-Savellano, E. Bos, C. Blondet, F. Sato, T. Abe, L. Josephson, R. Weissleder, J. Gaudet, D. Sgroi, P. J. Peters, J. P. Basilion, *Neoplasia* **2003**, *5*, 495-506.

[15] G. Sava, A. Bergamo*, Int. J. Oncol.* **2000**, *17*, 353-365.

[16] A. Ando, I. Ando, T. Hiraki, K. Hisada, *Int. J. Rad. Appl. Instrum*. B. **1988**, *15*, 133-140.

[17] P. Som, Z. H. Oster, K. Matsui, G. Guglielmi, B. R. Persson, M. L. Pellettieri, S. C. Srivastava, P. Richards, H. L. Atkins, A. B. Brill, *Eur. J. Nucl. Med. Mol. Imaging* **1983**, *8*, 491-494.

[18] S. C. Srivastava, P. Richards, G. E. Meinken, S. M. Larson, Z. Grunbaum, presented in part at *the Radiopharmaceuticals: structure activity relationships* symposium, Hartford, CT, USA, **1980**.

[19] W. Guo, W. Zheng, Q. Luo, X. Li, Y. Zhao, S. Xiong, F. Wang, *Inorg. Chem.* **2013**, *52*, 5328-5338.

[20] M. A. Jakupec, M. Galanski, V. B. Arion, C. G. Hartinger, B. K. Keppler, *Dalton Trans.* **2008**, 183-194.

[21] H. Yamada, T. Koike, J. K. Hurst, *J. Am. Chem. Soc*. **2001**, *123*, 12775-12780.

[22] M. J. Bloemink, J. Reedijk, *Met. Ions Biol. Syst.* **1996**, *32*, 641-685.

[23] J. Reedijk, *Proc. Natl. Acad. Sci. U.S.A.* **2003**, *100*, 3611-3616.

[24] F. Wang, A. Habtemariam, E. P. L. van der Geer, R. Fernández, M. Melchart, R. J. Deeth, R. Aird, S. Guichard, F. P. A. Fabbiani, P. Lozano-Casal, I. D. H. Oswald, D. I. Jodrell, S. Parsons, P. J. Sadler, *Proc. Natl. Acad. Sci. U.S.A.* **2005**, *102*, 18269-18274.

[25] E. S. Antonarakis, A. Emadi, *Cancer Chemother. Pharmacol.* **2010**, *66*, 1-9.

[26] W. Han Ang, P. J. Dyson*, Eur. J. Inorg. Chem.* **2006**, *2006*, 4003-4018.

[27] B. Therrien, *Coord. Chem. Rev*. **2009**, *253*, 493-519.

[28] A. Weiss, X. Ding, J. R. van Beijnum, I. Wong, T. J. Wong, R. H. Berndsen, O. Dormond, M. Dallinga, L. Shen, R. O. Schlingemann, R. Pili, C. M. Ho, P. J. Dyson, H. van den Bergh, A. W. Griffioen, P. Nowak-Sliwinska, *Angiogenesis* **2015**, *18*, 233-244.

[29] (a) M. Gras, B. Therrien, G. Süss-Fink, A. Casini, F. Edafe, P. J. Dyson, *J. Organomet. Chem.* **2010**, *695*, 1119-1125; (b) O. Renier, C. Deacon-Price, J. E. B. Peters, K. Nurekeyeva, C. Russon, S. Dyson, S. Ngubane, J. Baumgartner, P. J. Dyson, T. Riedel, H. Chiririwa, B. Blom, *Inorganics* **2017**, *5*, 44; (c) P. Buglyo, E. Farkas, *Dalton Trans.* **2009** *(38)*, 8063–8070; (d) L. C. Matsinha, P. Malatji, A. T. Hutton, G. A. Venter, S. F. Mapolie, G. S. Smith, *Eur. J. Inorg. Chem.* **2013**, *2013*, 4318-4328; (e) J. Soleimannejad, C. White, *Organometallics* **2005**, *24(10),* 2538–2541.

[30] See as an example of recently prepared Ru(II) trichlorogermyl complexes by insertion of $GeCl_2$ into Ru-Cl bonds: G. Albertin, S. Antoniutti, J. Castro, F. Scapinello, *J. Organomet. Chem.* **2014,** *751*, 412–419.

[31] E. Hodson, S. J. Simpson, *Polyhedron* **2004**, *23*, 2695-2707.

[32] S. Chari, University of Maastricht, unpublished work.

[33] C. Scolaro, C. G. Hartinger, C. S. Allardyce, B. K. Keppler, P. J. Dyson, *J. Inorg. Biochem.* **2008**, *102*, 1743-1748.

[34] C. Gossens, A. Dorcier, P. J. Dyson, U. Rothlisberger, *Organometallics* **2007**, *26*, 3969-3975.

[35] E. Wiberg, N. Wiberg, A. F. Holleman, *Inorganic chemistry, Academic Press* ; De Gruyter, San Diego; Berlin; New York, **2001**.

[36] (a) L. W. Pineda, V. Jancik, H. W. Roesky, D. Neculai, A. M. Neculai, *Angew. Chem. Int. Ed.* **2004**, *43*, 1419-1421; (b) G. Albertin, S. Antoniutti, J. Castro, *Eur. J. Inorg. Chem.* **2012,** *2012,* 4327-4333. (c) P. D. W. Boyd, M. C. Hart, J. R. F. Pritzwald-Stegmann, W. R. Roper,L. J. Wright, Organometallics **2012**, *31*, 2914−2921

[37] M. Hanif, S. M. Meier, W. Kandioller, A. Bytzek, M. Hejl, C. G. Hartinger, … B. K. Keppler, *J. Inorg. Biochem*. **2011**, *105(2)*, 224–231.

[38] P. Zhang, P. J. Sadler, *J. Organomet. Chem.* **2017**, *839*, 5–14.

[39] A. Tzubery, E. Y. Tshuva, *Eur. J. Inorg. Chem*. **2017**, *2017*, 1695-1705.

[40] (a) Gussian 09, Revision E.01, M. J. Frisch, G. W. Trucks, H. B. Schlegel, G. E. Scuseria, M. A. Robb, J. R. Cheeseman, J. A. Montgomery, Jr., T. Vreven, K. N. Kudin, J. C. Burant, J. M. Millam, S. S. Iyengar, J. Tomasi, V. Barone, B. Mennucci, M. Cossi, G. Scalmani, N. Rega, G. A. Petersson, H. Nakatsuji, M. Hada, M. Ehara, K. Toyota, R. Fukuda, J. Hasegawa, M. Ishida, T. Nakajima, Y. Honda, O. Kitao, H. Nakai, M. Klene, X. Li, J. E. Knox, H. P. Hratchian, J. B. Cross, V. Bakken, C. Adamo, J. Jaramillo, R. Gomperts, R. E. Stratmann, O. Yazyev, A. J. Austin, R. Cammi, C. Pomelli, J. W. Ochterski, P. Y. Ayala, K. Morokuma, G. A. Voth, P. Salvador, J. J. Dannenberg, V. G. Zakrzewski, S. Dapprich, A. D. Daniels, M. C. Strain, O. Farkas, D. K. Malick, A. D. Rabuck, K. Raghavachari, J. B. Foresman, J. V. Ortiz, Q. Cui, A. G. Baboul, S. Clifford, J. Cioslowski, B. B. Stefanov, G. Liu, A. Liashenko, P. Piskorz, I. Komaromi, R. L. Martin, D. J. Fox, T. Keith, M. A. Al- Laham, C. Y. Peng, A. Nanayakkara, M. Challacombe, P. M. W. Gill, B. Johnson, W. Chen, M. W. Wong, C. Gonzalez, and J. A. Pople, Gaussian, Inc., Wallingford CT, **2004**; (b) A. D. Becke, *J. Chem. Phys.* **1993**, *98*, 5648; (c) C. Lee, W. Yang, R. G. *Parr, Phys. Rev. B* **1988**, *37,* 785; (d) B. Miehlich, A. Savin, H. Stoll, H. Preuss, *Chem. Phys. Lett.* **1989,** *157,* 200.

TOC Image

A series of trichlorogermyl complexes of the type [η^6-(Arene)Ru(PR_3)Cl($GeCl_3$)], including full spectroscopic characterisation are reported and their cytotoxicity towards A2780 or HEK293 cell lines are also reported along with DFT studies.